



Supporting Online Material for

Polarized Myosin Produces Unequal-Size Daughters During Asymmetric Cell Division

Guangshuo Ou,^{*} Nico Stuurman, Michael D'Ambrosio, Ronald D. Vale^{*}

^{*}To whom correspondence should be addressed. E-mail: gou@ibp.ac.cn (G.O.);
vale@cmp.ucsf.edu (R.D.V.)

Published 30 September 2010 on *Science Express*
DOI: 10.1126/science.1196112

This PDF file includes:

Materials and Methods
Figs. S1 to S8
Table S1
References

Other Supporting Online Material for this manuscript includes the following:
(available at www.sciencemag.org/cgi/content/full/science.1196112/DC1)

Movies S1 to S10

Materials and Methods

Strains

C. elegans strains were raised on NGM plate seeded with the *Escherichia coli* strain OP50 at 20°C using standard methods. Wild-type animals were of Bristol variety N2 strain. Strains bearing mutations or transgenic arrays obtained from Caenorhabditis Genetics Center are the following. JJ1473; unc-119(ed3) III; zuls45[nmy-2::NMY-2::GFP + unc-119(+)] V. NG4370; zdIs5[mec-4::GFP + lin-15(+)] I; pig-1(gm344) IV . NG5431; ced-4(n1162) III; him-5(e1490) V; ayls9[egl-17::NLS::GFP + dpy-20 (+)] V. TH27; unc-119(ed3) III; ddIs6[tbg-1::GFP + unc-119(+)]. CF693; unc-31(e169) IV; him-5(e1490) V; muls28[mig-2::GFP + unc-31(+)]. Strains made in this study are the following: RDV55; rdvIs1[*Pegl-17::mCherry::his-24+Pegl-17::myristoylated mCherry + Pegl-17::mig-10::yfp+ pRF4*]. RDV53; rdvEx53[*Pegl-17::myristoylated mCherry + Pegl-17::EBP-2::gfp+ pRF4*]. RDV70; rdvEx70[*Pegl-17::myristoylated mCherry + Pegl-17::mCherry::his-24+Pegl-17::TBA-2::gfp+ pRF4*]. RDV83 (rdvIs1; zuls45 V) was made by crossing RDV55 males with JJ1473 hermaphrodite. RDV84 (rdvIs1; ddIs6) was made by crossing RDV55 males with TH27 hermaphrodite. RDV200 (zdIs5 I; rdvIs1; *pig-1(gm344)* IV; zuls45 V) was made by crossing RDV83 males with NG4370.

Molecular Biology and Transgenesis

PCR fusion techniques were used to generate mCherry reporters of Q cell plasma membrane and chromosomes. We used the *egl-17* promoter to drive coding regions for Q cell specification expression. All fusions were performed by either Phusion DNA polymerase (New England Biolabs) or the AccuPrime Pfx SuperMix (Invitrogen). PCR templates and primers are listed Table S1.

Transgenic *C. elegans* were created by germline transformation. PCR products were co-injected into N2 hermaphrodites at 5 ng/μl with 50 ng/μl pRF4, except that *Pegl-17::MYR-mecherry* was injected at 15

ng/ μ l to make RDV53. RDV55 was spontaneously integrated into the genome. Although MIG-10::YFP was co-injected, it only shows fluorescence at the birth of QR.a/p cells and is not visible during their divisions. The NMY-2::GFP construct was transformed using microparticle bombardment (S1), which results in low copy integration and low protein expression close to the endogenous level. The NMY-2::GFP strain used in our work has been widely used in studying various cell biological questions in *C. elegans* embryos and germ line, and protein over expression causes silencing in the *C. elegans* germline, suggesting that NMY-2::GFP cannot be over expressed. Moreover, NMY-2::GFP can rescue the sterile phenotype in a *nmy-2* deletion mutant (personal communication with Drs. Nance and Priess). Although NMY::GFP was expressed in the wild type background, GFP tagged myosin is at least 50% of the total myosin because particle bombardment transformation can deliver one or several copies of GFP tagged NMY-2 into *C. elegans* genome. Since wildtype and GFP tagged myosins coassemble into filaments, CALI can have a phenotypic effect on myosin function.

Q Cell Imaging

Microscopy methodology for visualizing Q neuroblast asymmetric cell division was modified from our recent technique of studying Q cell migration (S2). In brief, *C. elegans* L1 larva were anesthetized with 0.1 mM levamisole in M9 buffer, mounted on 2% agar pads, and maintained at 22°C. Our imaging system includes an Axiovert 200M microscope (Carl ZeissMicroImaging, Inc.) equipped with a 100X, 1.45 N.A. objective, an EM CCD camera (Hamamatsu model, C9100-13), and the 488 nm and 568 nm lines of an Argon and Krypton laser attached to a spinning disk confocal scan head (Yokogawa CSU10 obtained from Solamere Inc.). Time-lapse images were acquired with exposure time of 300 msec at every 20 sec by μ Manager (www.micro-manager.org) software. To image membrane dynamics by MYR-mCherry in strain RDV53, the exposure time was 500 msec and images were taken at every 5 sec.

Chromophore-assisted laser inactivation (CALI)

We modified the optics in the Zeiss Axiovert 200m microscope to allow both CALI and spinning disk confocal acquisition. For chromophore-assisted laser inactivation (CALI), we focused the 488 nm line of an argon laser (Model, 35-LAP-431-208R, Melles Griot, Carlsbad, CA) in a diffraction limited spot in the sample by using a second optical fiber that coupled the laser light to a Zeiss TIRF slider installed in the slot for the field diaphragm of the epi-illumination path. Light output was switched between the two fibers using a polarizing beam splitter and insertion of a half wave plate controlled by the μ Manager software using a servo. The light was focused on the sample rather than the back-focal plane of the objective by inserting a biconcave lens (Optosigma 017-0275, D=25.40, focal length of 89.7 mm) into the reflector cube at the position of the emission filter along with either a 488 nm reflecting long pass mirror or a 100% reflecting mirror in the cube. The laser spot was focused using the focus control on the TIRF slider while observing a coverslip coated with the lipophilic carbocyanine dye DiI. Spot size was estimated to be 1 μ m in diameter, causing an excitation power of 2 mW (power measured at the end of the fiber) to result in a power density of about 250 kW cm⁻² at the sample. Switching time between CALI and spinning disk modalities was only limited by reflector turret movement and was on the order of 300 msec.

To maximize the efficiency of finding mitotic QR.a or QR.p cells for CALI, we synchronized *C. elegans* by allowing ~100 adults to lay eggs for 1-2 hr, removing the adults, and then incubating the eggs at 22°C for 16 hr to obtain L1 larvae. We then recorded multiple (~5) migrating QR.a and QR.p cells from different larvae using multi-position acquisition with images in each field acquired at 90 sec intervals. When we identified a cell that enters mitosis, we stopped multi-position acquisition and imaged the mitotic cell every 5 sec. If a mitotic QR.a or QR.p cells was not identified within 2 hr, the sample was discarded. During the acquisition of a mitotic cell, we frequently paused to adjust the focus and moved the anterior portion of QR.a cell (or the posterior of QR.p cell in control experiments) into the focus of the CALI illumination (~ 1 μ m, as described above). CALI was performed at the onset of cytokinesis, as identified

by the separation of the mCherry-histone fluorescence (sister chromatid separation). The 488 nm CALI illumination was applied one time for 300 msec on one side of QR cell (Fig. S7B), or the anterior of QR.a cell and the posterior of QR.p cell three times for 300 msec at 5 sec intervals (Fig. 3). After CALI, we switched to acquiring images of the ensuing Q cell division every 5 sec. To follow the cell fate of QR.aa cell, we imaged them at about 3 hr after division or took time-lapse movies by imaging every 90 sec for about 3 hr, occasionally adjusting the position and focus of the stage to keep the cell in view. Apoptotic cells were those whose fluorescence either disappeared entirely or formed a very small round shape characteristic of a dying cell. A survival cell had a normal spread out shape, and a subset also extended a long process 150 min after birth.

Fluorescence Quantifications

We used ImageJ software (<http://rsbweb.nih.gov/ij/>) and Adobe Photoshop CS3 to process images. Fluorescence quantifications were performed by ImageJ software. To calculate the ratio of anterior/posterior centrosome to cell center distances in Fig. 1B, we used ImageJ to measure the distance between gamma-tubulin (TBG-1::GFP) to the middle of cell (MYR-mCherry). Representative frames at the metaphase and anaphase transition of QR.a or QR.p division are presented in Fig. 1B and Fig. S3, and those for QL.a or QL.p cells are in Fig. S2A.

We used mCherry-labeled plasma membrane and histone markers to determine the position of furrow. In time-lapse movies, after chromosomes are segregated at late anaphase, the furrow is defined as the line connecting the points where the membrane is invaginating to an apex on either side of the cell. The accumulation of GFP tagged myosin II along this line confirms this to be the position of the furrow.

We used two independent approaches to determine if there is any asymmetric distribution of myosin II (NMY-2::GFP) in WT QR.a and QR.p or WT QL.a and QL.p or *pig-1(gm344)* mutant QR.a cells during cytokinesis. The first approach calculated the myosin II distribution ratio between anterior and

posterior part of the cell (Fig. 2B and Fig. S2C-D). Plasma membrane marker (MYR-mCherry) was used to find the cleavage plane, and ImageJ was used to circumscribe the fluorescence field and measure the sizes of area with GFP fluorescence in the anterior or posterior part of the contractile ring. Over two independent measurements of the same set of images by different individuals without knowing cell types and genetic backgrounds were averaged and presented in Fig. 2B and Fig. S2D.

The second approach used a custom Matlab program to assess any inherent asymmetry in the myosin distribution across the cleavage plane in an unbiased manner that required very little human input (Fig. S4A). The algorithm has two steps: The first step is to identify the relevant signal and centroid of this signal, and the second step is to calculate the maximum axis of symmetry intersecting this centroid. First, relevant myosin signal is identified by applying a $1.5 \times$ background pixel level threshold (background level is determined from an area of background selected by the user). Second, the grayscale-weighted centroid of the myosin signal is identified. Third, a line is drawn by the user, intersecting the centroid, bisecting the image into two images (image 1 and image 2). This bisecting line is rotated by one degree from -10 to +10 degrees from the starting position, and symmetry values are calculated between image one and the mirror-image of image 2 by position-by-position subtraction. Asymmetry was calculated by adding up all pixels which did not contain myosin II in the mirror image. The line across which asymmetry is minimized is the final value. The purpose of starting with the user selected line and defining a limited range around this line is to avoid measuring the symmetry of the myosin distribution across the axis perpendicular to the cleavage plane, which will be retained even given an asymmetric distribution of myosin across the cleavage plane.

Student's *t*-Tests were used to examine statistical differences of myosin II distribution between QR.a and QR.p in WT or QR.a between WT and *pig-1 (gm344)* mutant.

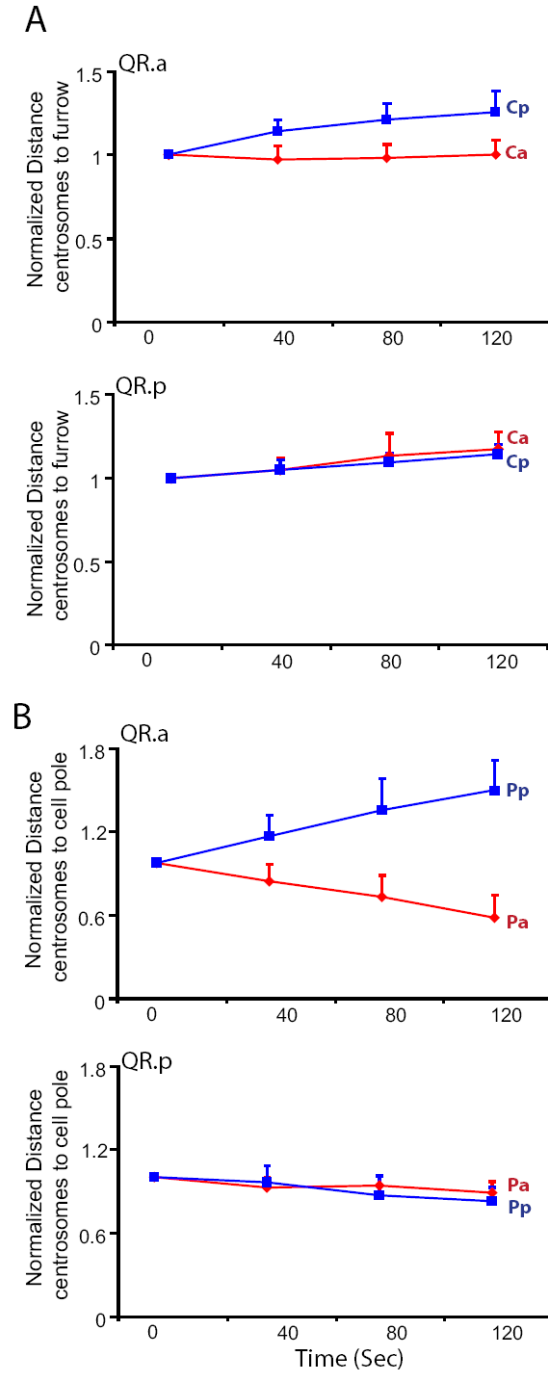


Fig. S1 Asymmetry of spindle elongation during Q neuroblast divisions.

A) and B) Quantifications of centrosome to furrow distance (**A**) and cell pole distance (**B**) from 10 movies. Data is normalized compared to the initial distances for each centrosome at the start of anaphase. Error bars indicate mean \pm SD. Spindle asymmetry (Ca/Cp) in the QR.a cell arises from the constant length of Ca but elongation of Cp, and the daughter cell size asymmetry in QR.a results from the shrinkage of anterior pole (Pa) towards the centrosome and expansion of the posterior pole (Pp) away from the centrosome.

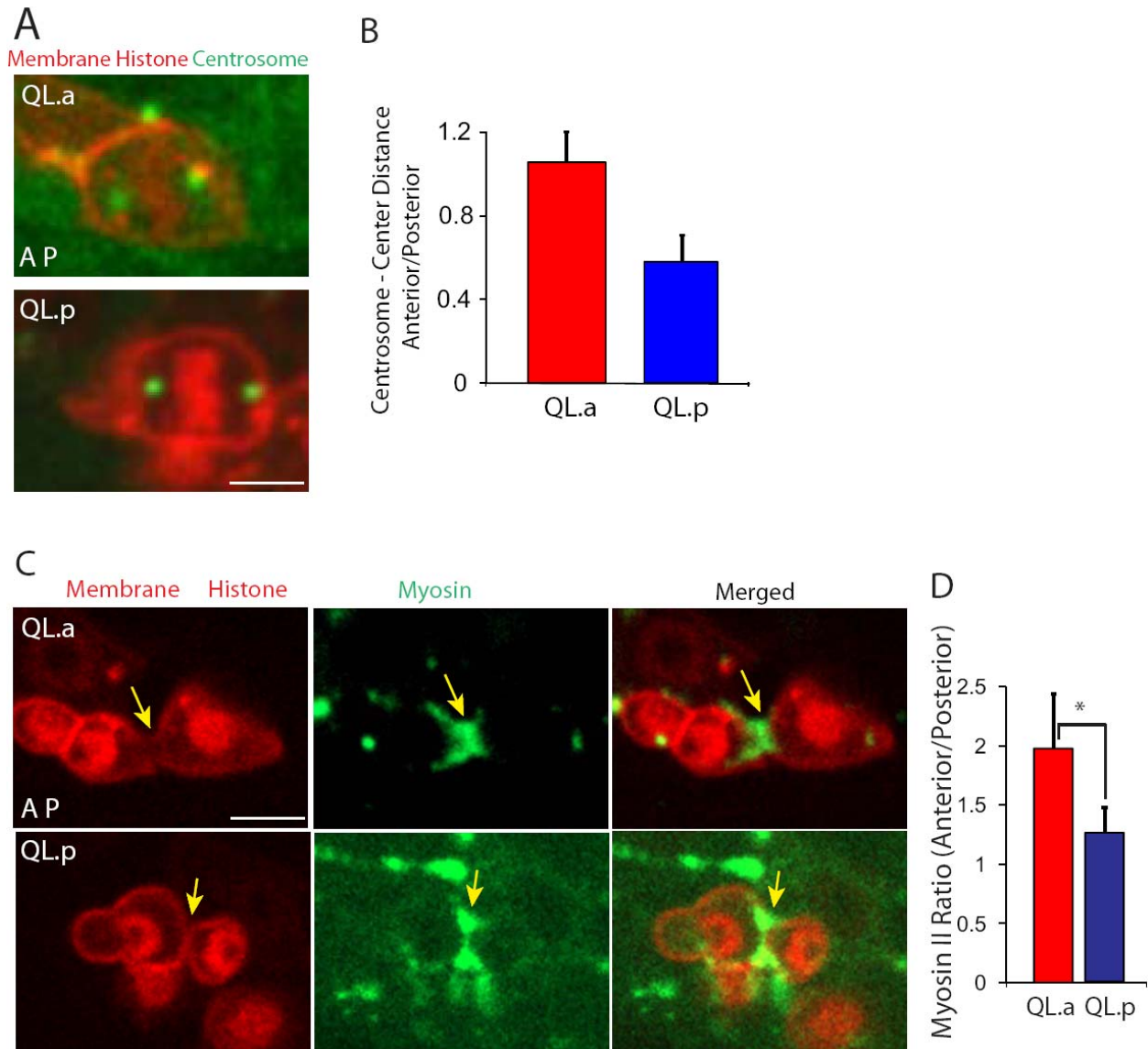


Fig. S2. Spindle positioning and myosin II distribution in asymmetric cell division of QL.a and QL.p

A) Spindle positioning in the second round asymmetric cell division of QL.a and QL.p cells with centrosomes (gamma-tubulin, TBG-1::GFP) in green and plasma membrane (mCherry with a myristoylation signal) and histone (his-24::mCherry) in red. The anterior of the cell is towards the left. The spindle is displaced posteriorly in the QL.p cell but is centered in the QL.a cell. **B)** Centrosome-to-cell center distance ratio (anterior centrosome distance divided by posterior centrosome distance). Error bars indicate mean \pm SD (n=10). Cell center is defined as the midpoint between the two cell poles. **C)** Images of myosin II-GFP in QL.a (upper) and QL.p (lower) animals. **D)** Myosin II-GFP fluorescence intensities ratio between the anterior and posterior parts of QL.a and QL.p (*, $p < 0.001$, n=9-11). Error bars indicate mean \pm SD.

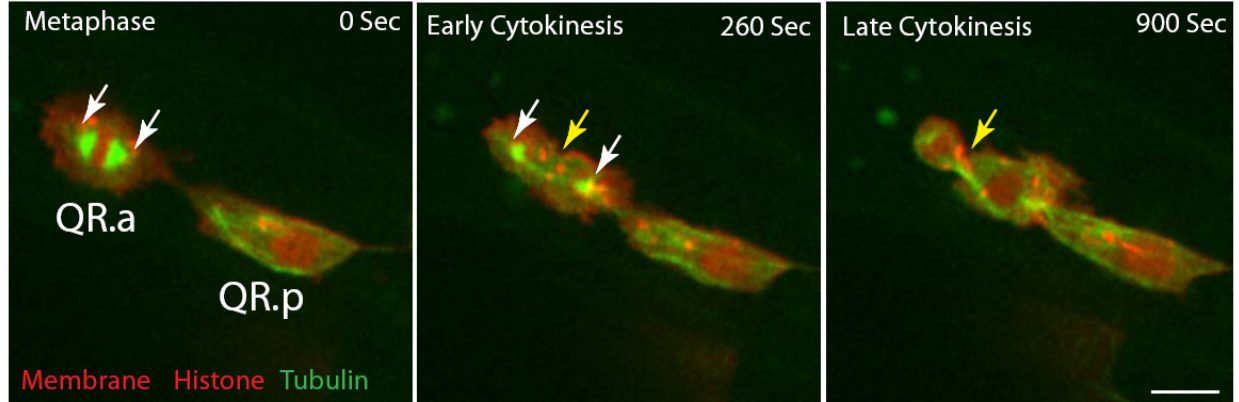
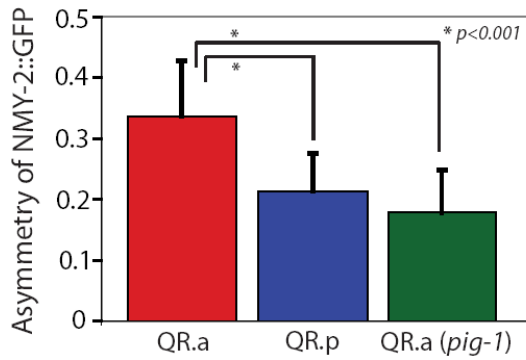


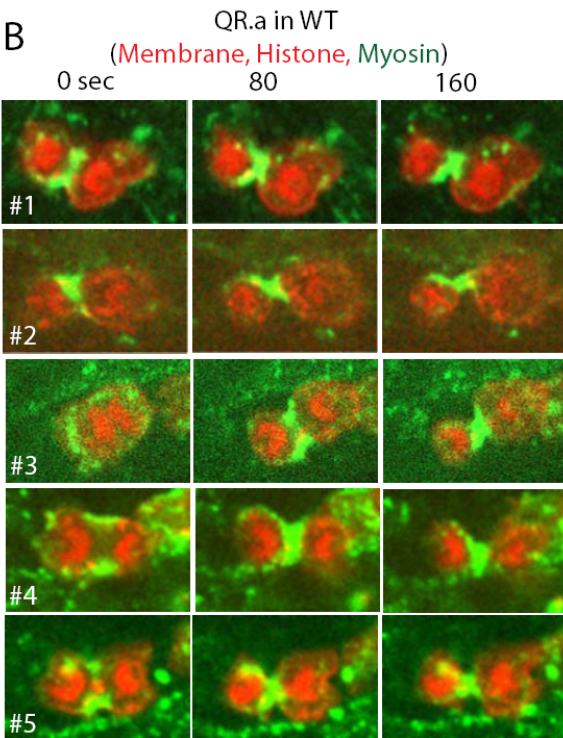
Fig. S3. Spindle in the QR.a cell during asymmetric cell division.

Spindle in QR.a cell is visualized by GFP tagged alpha-tubulin (TBA-2). Plasma membrane and histone are labeled by mCherry. Anterior of the cell is towards left. White arrows point to the spindle poles. Spindle is positioned in the center of QR.a cell in metaphase (left) and the cleavage furrow (yellow arrow) is initiated in the center of spindle (middle) in early cytokinesis.

A



B



C

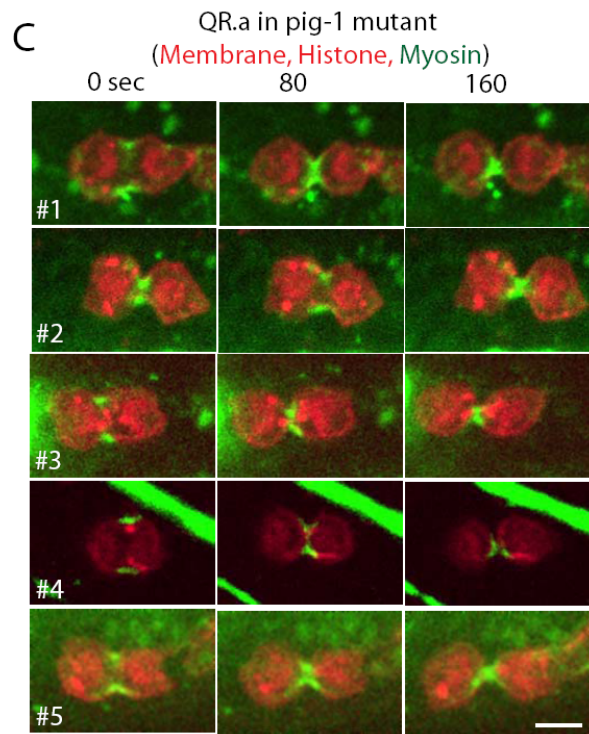


Fig. S4 Asymmetry of myosin II in QR.a cells.

A) Myosin II (NMY-2::GFP) in the contractile ring of WT QR.a or QR.p cells or *pig-1* (*gm344*) mutant QR.a cells ($n=9-11$). Error bars indicate mean \pm SD. The asymmetry is determined by a custom Matlab program, and Y axis shows minimum asymmetry of myosin signal bisected through the centroid (see Methods). **B)** and **C)** Frames from 5 different time lapse movies of QR.a cell cytokinesis from WT (**B**) or *pig-1* (*gm344*) mutant (**C**) animals. Plasma membrane and histone are labeled by mCherry in red. Myosin II is labeled by GFP in green. Times in second are indicated. Anterior of cell is towards the left. Bar = 2.5 μ m.

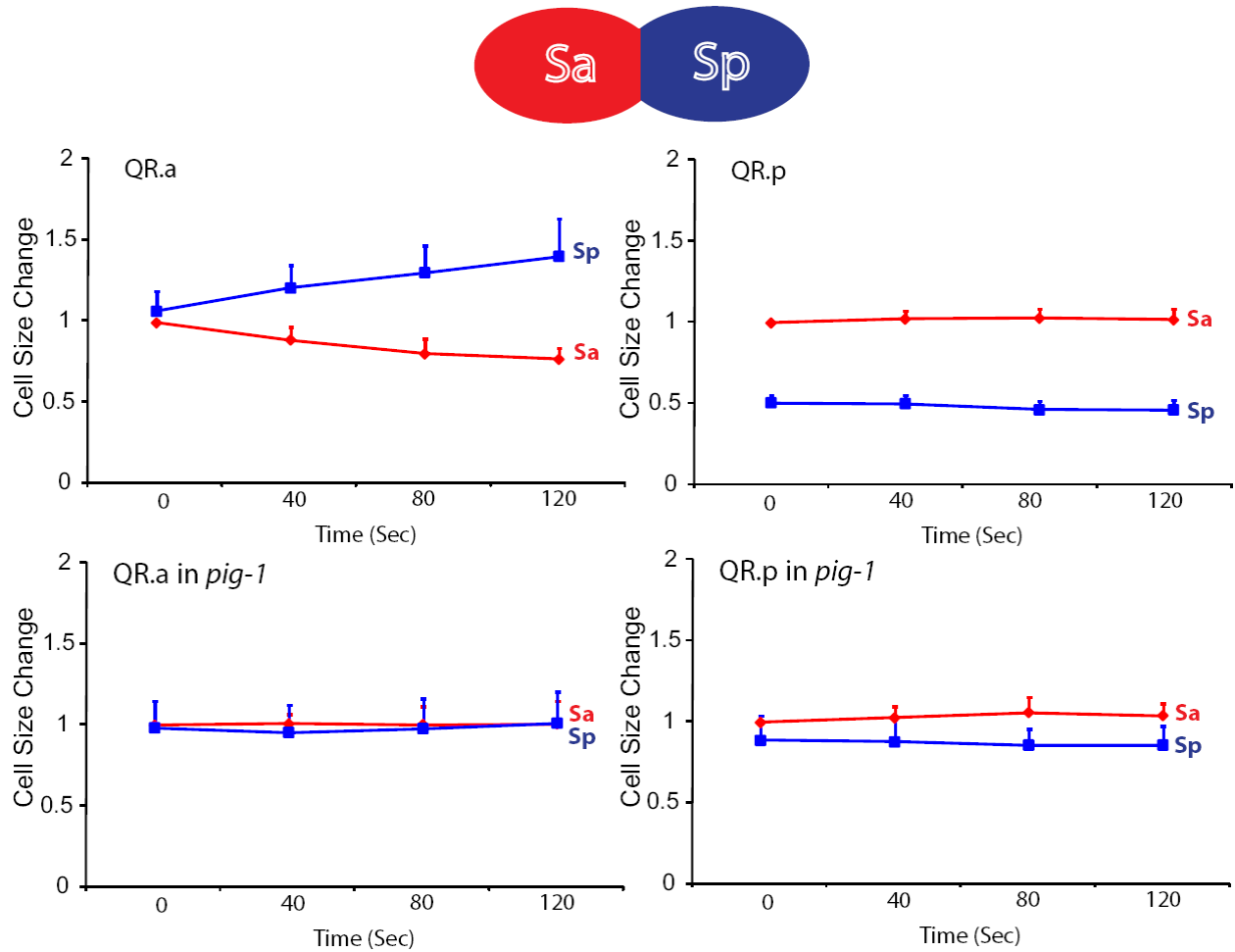


Fig. S5 Daughter cell size change during cytokinesis.

QR.a cell (upper left) gradually shrinks the anterior half and enlarges the posterior half, resulting in two daughter cells of distinct sizes. Sa is the size of the anterior and Sp is the size of the posterior of dividing Q cells. The anterior portion of QR.p cell (upper right) is twice as large as the posterior at the start of cytokinesis, and the anterior over posterior cell size ratio remains constant until the end of division. In *pig-1* mutant, QR.a (lower left) and QR.p (lower right) maintain the same anterior and posterior sizes, resulting in two daughter cells of similar sizes after division. Size is determined by bisecting the cell at the position of the cleavage furrow and measuring the area to the left (anterior) and right (posterior). Time 0 sec is the start of furrow formation. Error bars indicate mean \pm SD (n=10).

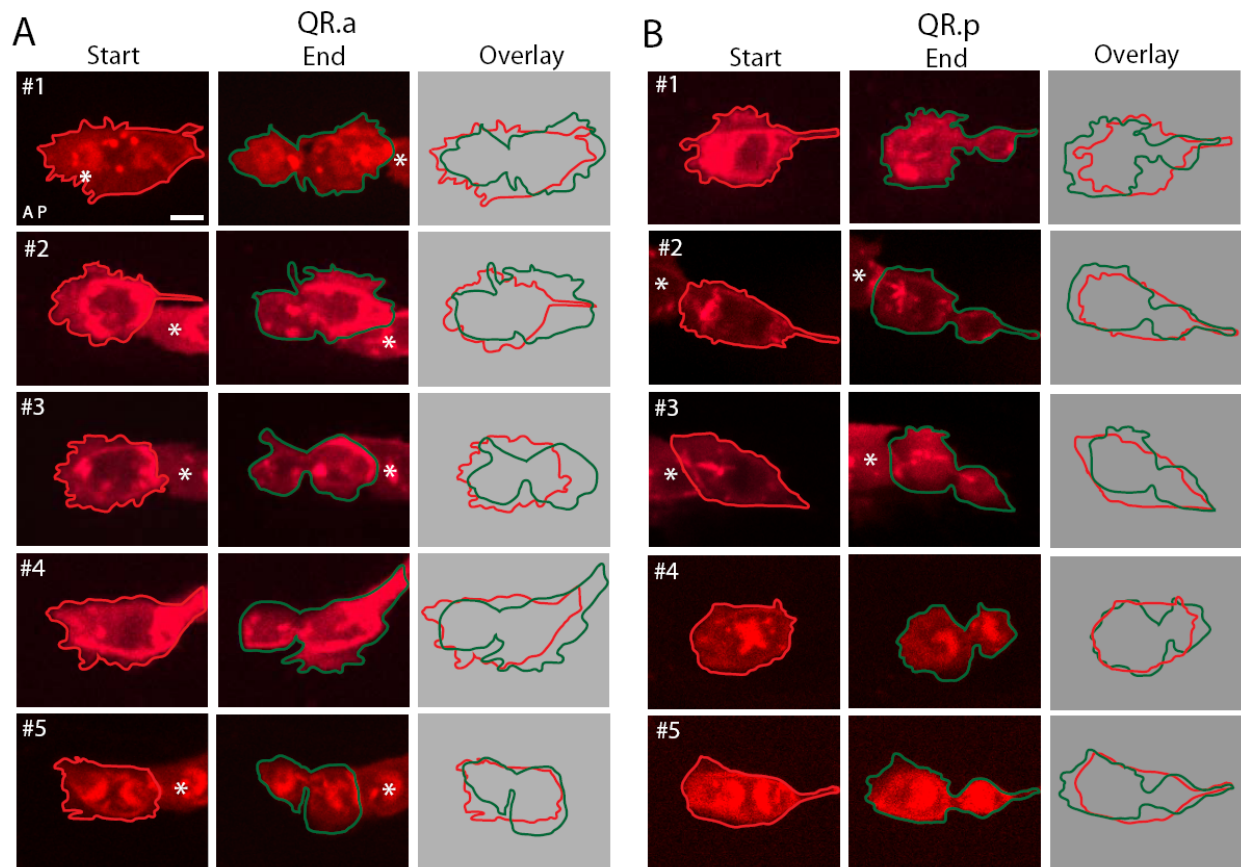


Fig. S6 Membrane morphology of QR.a and QR.p cells during cytokinesis.

A) and **B)** More examples of still images from five different time-lapse movies showing membrane morphology of QR.a (**A**) and QR.p (**B**) at the start and the end of cytokinesis. Anterior of the cell is left. Asters show neighboring Q cells. Bar = 2.5 μm .

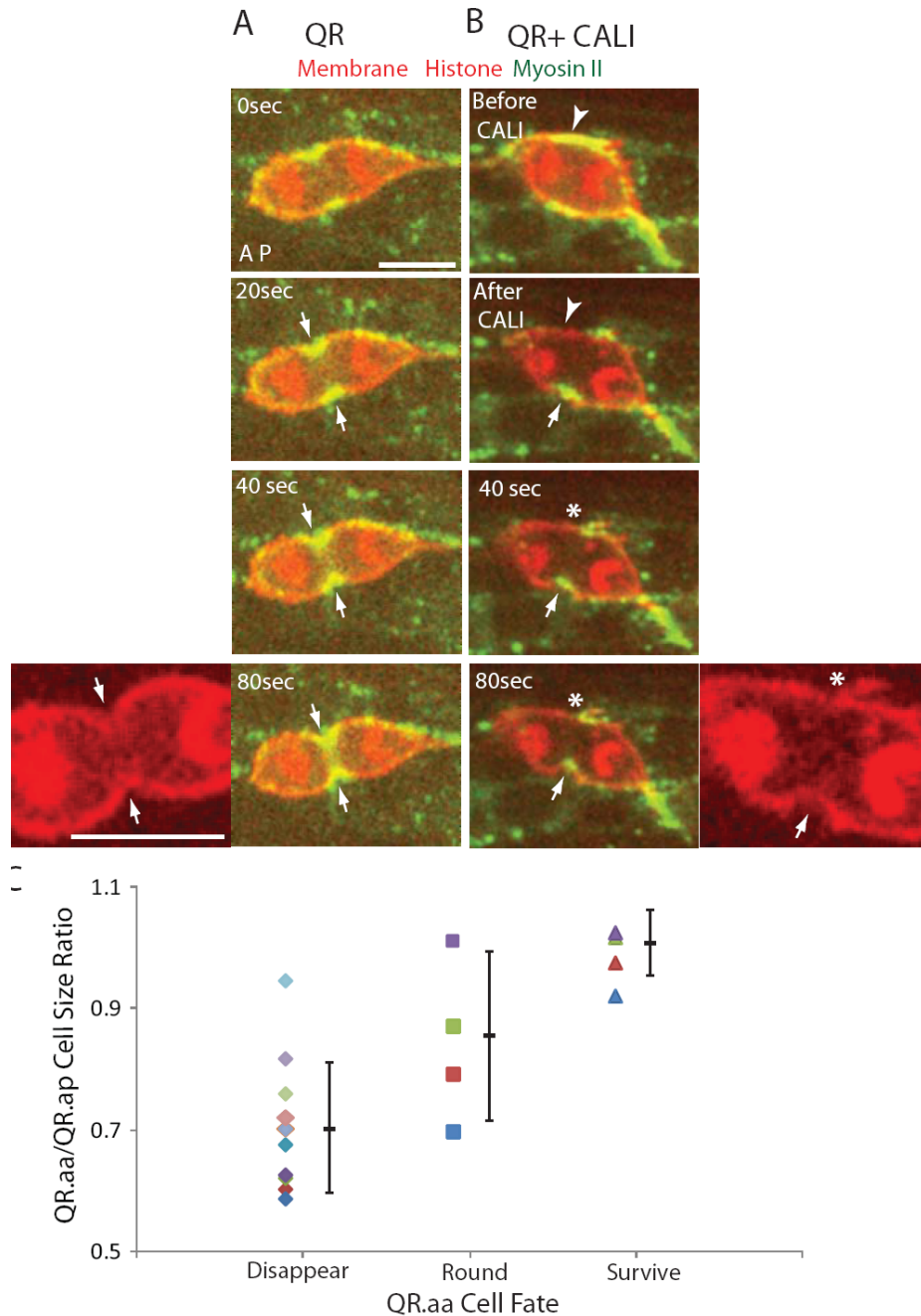


Fig. S7. CALI in QR and QR.a cells

A) QR neuroblast normally undergoes equal cell division and cleavage furrows on both sides (white arrow) initiate and progress evenly during cytokinesis. **B)** Furrow ingression is paused (asters) on the side of myosin II inactivation by CALI (arrow heads), while the furrow ingresses on the opposite side (arrows). The image on the left bottom in **A)** or right bottom in **B)** (plasma membrane and histone in red) provides a zoomed up view of furrow ingression from the neighboring frame (80sec). Anterior of the cell is left. Bar = 5 μ m. **C)** Plot of QR.aa/QR.ap cell size ratio and QR.aa cell fate after CALI. Error bars indicate mean \pm SD. The mean size of QR.aa cells that survive after CALI is larger than the size of those that disappear ($p < 0.001$).

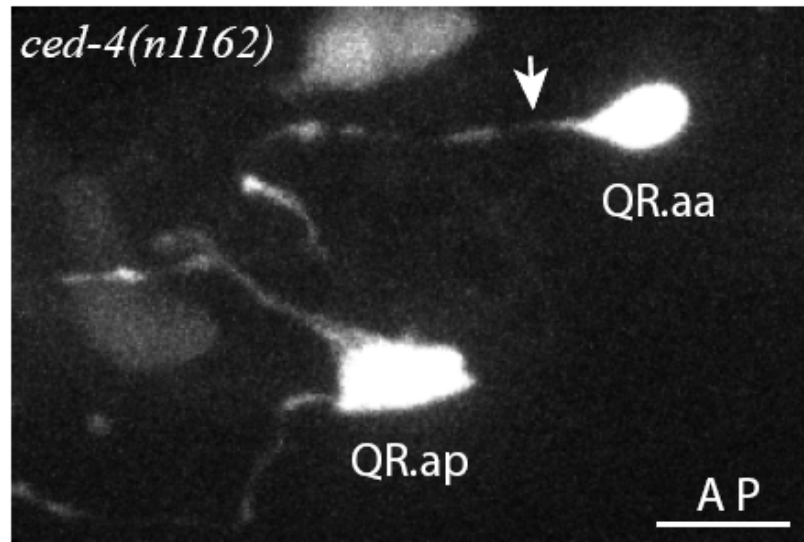


Fig. S8. Neurite-like structure formation of QR.aa cell in apoptosis mutant

In *ced-4(n1162)* mutant, QR.aa cell survived and formed neurite-like structure (75%, N=12; pointed by an arrow). Anterior of the cell is left. Bar = 5 μ m.

Table S1 PCR Reactions

PCR Product	Primer 5'	Primer 3'	Template
egl-17 promoter	CAGATGGATG TTTACTGCCA ACTGG	AGCTCACATT TCGGGCACCT GAA	N2 Genomic DNA
MYR-mCherry	CAGGTGCCCCGAAATGTGAGCT ATGGGTTCTT GTATTGGAAA AGTCTC	CTAAAGGGAA CAAAAGCTGG AGC	pJWZ50.3
mCherry	CAGGTGCCCCGAAATGTGAGCT ATG GTC TCAAAGGGTG AAGAAGATAA C	AGTACCTCCACCTCCGCTG TCCATGT	pAA65
EBP-2	ACATGGACAGCGGAGGTGGAGGTAC T ATGGTCGTCA ACGTGTTTCA C	GCGATTCCTT GTTTATTTCC AAGGC	N2 Genomic DNA
his-24	ACATGGACAGCGGAGGTGGAGGTAC T ATGTCTGATT CCGCTGTTGT TGC	CAATGTTTAT TGAAGACGTT GAACGTC	N2 Genomic DNA
TBA-2	ACATGGACAGCGGAGGTGGAGGTAC T ATGCGTGAGG TCATCTCTAT CC	CGCTTTTAA GGCAAAAAAG GAG	N2 Genomic DNA
Pegl-17::MYR- mCherry	CTTCCGTTCT ATGGAACACT C	GAATCATCGT TCACTTTTCA CGG	egl-17 promoter + MYR-mCherry
Pegl-17:: mCherry::his-24	CTTCCGTTCT ATGGAACACT C	GAAGACGTTG AACGTCAAAT TATC	egl-17 promoter + mCherry + his-24

Supplementary movie legends:

Video S1

Spindle positioning and elongation in dividing QR.p cell. Centrosome in green, chromosome and plasma membrane in red (Strain RV83). The display rate is 7 frames/sec with total elapsed time of 960 sec. Anterior, left.

Video S2

Spindle positioning and elongation in dividing QR.a cell. Centrosome in green, chromosome and plasma membrane in red (Strain RV83). The display rate is 7 frames/sec with total elapsed time of 1212 sec. Anterior, left.

Video S3

Spindle positioning and elongation in dividing QR.a cell. Microtubules in green, chromosome and plasma membrane in red (Strain RV70). The display rate is 7 frames/sec with total elapsed time of 1680 sec. Anterior, left.

Video S4

Myosin II dynamics in cytokinetic QR.p cell. Myosin II in green, chromosome and plasma membrane in red (Strain RV84). The display rate is 7 frames/sec with total elapsed time of 460 sec. Anterior, left.

Video S5

Myosin II dynamics in cytokinetic QR.a cell. Myosin II in green, chromosome and plasma membrane in red (Strain RV84). The display rate is 7 frames/sec with total elapsed time of 480 sec. Anterior, left.

Video S6

Membrane dynamics in dividing QR.p cell. Plasma membrane in red (Strain RV53). The display rate is 15 frames/sec with total elapsed time of 955 sec. Anterior, left.

Video S7

Membrane dynamics in dividing QR.a cell. Plasma membrane in red (Strain RV53). The display rate is 15 frames/sec with total elapsed time of 935 sec. Anterior, left.

Video S8

Myosin II dynamics in cytokinetic QR.a cell of *pig-1* mutant. Myosin II in green, chromosome and plasma membrane in red (RV200). The display rate is 5 frames/sec with total elapsed time of 460 sec. Anterior, left.

Video S9

QR.aa cell undergoes programmed cell death. Aster is adjacent to QR.aa cell. Chromosome and plasma membrane in red. The display rate is 7 frames/sec with total elapsed time of 111 min. Anterior, left.

Video S10

QR.aa cell migrates and forms neuritis after CALI of myosin II during cytokinesis. Aster is adjacent to QR.aa cell. Chromosome and plasma membrane in red. The display rate is 7 frames/sec with total elapsed time of 165 min. Anterior, left.

Supplemental References

- S1. J. Nance, E. M. Munro, J. R. Priess, *Development* **130**, 5339 (Nov, 2003).
- S2. G. Ou, R. D. Vale, *J Cell Biol* **185**, 77 (Apr 6, 2009).